agriculture

MDPI

Article

Behavioral Analysis of Mowing Workers Based on Hilbert–Huang Transform: An Auxiliary Movement Analysis of Manual Mowing on the Slopes of Terraced Rice Fields

Bo Wu [1,†], Yuan Wu [2,†], Ran Dong [1,*], Kiminori Sato [1], Soichiro Ikuno [1], Shoji Nishimura [2] and Qun Jin [2]

[1] School of Computer Science, Tokyo University of Technology, 1404-1 Katakuramachi, Hachioji, Tokyo 192-0982, Japan
[2] Advanced Research Center for Human Sciences, Waseda University, 2-579-15 Mikajima, Saitama Prefecture, Tokorozawa 359-1192, Japan
* Correspondence: randong@stf.teu.ac.jp
† These authors contributed equally to this work.

Abstract: In the mountainous areas of Japan, the weeds on the slopes of terraced rice paddies still need to be cut by the elderly manually. Therefore, more attention should be given to maintain proper postures while performing mowing actions (especially the pre-cutting actions) to reduce the risk of accidents. Given that complex mowing actions can be decomposed into different sub-actions, we proposed a joint angular calculation-based body movement analysis model based on the Hilbert–Huang transform to analyze the pre-cutting actions. We found that the two most important sub-actions were fast pre-cutting and slow pre-cutting. Based on field experiments, we analyzed the pre-cutting actions of workers with different experience levels and identified the factors that affected their falling risk (stability). The results showed differences and similarities in the actions' frequency and amplitude in the sub-actions of workers with different mowing experience, confirmed the influence of body characteristics (body height, etc.) on body stability, and showed that workers should pay attention to their age and ankle part while mowing. The analysis results have identified factors for the mowing workers' training and the development of equipment for use in complicated geographical conditions.

Keywords: agricultural work support; Hilbert–Huang transform method; body motion measurement; human behaviors analysis; pre-cutting analysis; mowing on slopes; empirical mode decomposition; visualization of agricultural experience

Citation: Wu, B.; Wu, Y.; Dong, R.; Sato, K.; Ikuno, S.; Nishimura, S.; Jin, Q. Behavioral Analysis of Mowing Workers Based on Hilbert–Huang Transform: An Auxiliary Movement Analysis of Manual Mowing on the Slopes of Terraced Rice Fields. *Agriculture* **2023**, *13*, 489. https://doi.org/10.3390/agriculture13020489

Academic Editor: Massimo Cecchini

Received: 26 January 2023
Revised: 14 February 2023
Accepted: 15 February 2023
Published: 18 February 2023

1. Introduction

A ridge is generally placed on the boundary of a paddy field to prevent irrigation water from leaking out. Some weeds can grow over 2 m tall, and if vegetation management is neglected, ventilation and lighting in paddy fields will be hindered [1]. In terraced rice fields, the range of ridges and slopes is wide. In Japan, paddy fields with a slope of 1/20 or more and fields, grasslands, and pastures with a slope of 15 degrees or more are defined as slope farmland [2]. Because of the difficult terrain, weeds on the ridges and slopes of terraced rice paddies still need to be cut manually using a handheld petrol mower [2]. The number of people engaged in agriculture has decreased from 1.755 million in 2005 to 1.226 million in 2022, during which the aging rate (the proportion of the population aged 65 years and over) has risen from 65% to 70% [3]. In particular, the hilly and mountainous areas are facing remarkable depopulation and aging; people over the age of 65 are responsible for many mowing works in these areas. The farmlands in mountainous areas in Japan, especially terraced rice fields, have steep slopes and many obstacles, such as pebbles. The Japanese government also has provided financial support for mowing the ridges and slopes of the farmland in hilly and mountainous areas since 2000. However, due to the

aging of the farming population, the farmers over the age of 65 in those areas have to mow the weeds on ridges and slopes by themselves. So, more research is needed to ensure the safety of the mowing works [4].

As a basic movement that requires the cooperation of whole-body muscles, the mowing action requires a combination of complex movements within a short time to complete the adjustment of body balance to prevent falls while increasing efficiency. According to a related survey [5], about 30% of accidents, including falls, slips, etc., are caused by workers' unstable posture. Improper postures can place a heavy burden on a worker's body, thus increasing the risk of accidents [6]. Therefore, an in-depth analysis of mowing workers' behaviors on slopes is necessary to determine their movement characteristics.

With the development of IoT-based technologies, human body movements can already be acquired well dynamically. One common method is the use of motion capture devices, such as the Xsens MVN, to record whole-body movements via accelerometer sensors [7]. However, due to the complexity of human actions, actions that appear to have the same purpose can be decomposed into different sub-actions, and these complex sub-actions may affect our analysis of the whole action.

The decomposition of motion features with varying action goals in the frequency domain has been extensively explored with human behavioral feature extraction techniques [8]. However, the traditional methods of Fourier Transform (FT) [9,10] and wavelet transform [11] have been found to be challenging to interpret and not ideal for the analysis of human actions. A more appropriate method for the decomposition of realistic actions is the Hilbert–Huang Transform (HHT), a non-linear and empirical technique [12–14].

In our previous studies [15,16], we analyzed the mowing action on slopes by using a motion capture technique with key joint angle analysis. However, we focused on the "kinetic energy release phase" (e.g., main "cutting" action) of the mowing workers and did not pay much attention to the "kinetic energy storage phase," the preparatory action that directly affects the quality of all "main" mowing actions.

Unlike the "main" mowing action, which swings by gravity and has only one purpose (i.e., "cutting"), the "cutting preparatory (pre-cutting) action" needs to balance at least three complex purposes of "maintaining body stability," "reserving kinetic energy," and "lifting the mower (trimmer machine)". Direct analysis of the limb joint movements during worker movements alone may not be comprehensive enough to avoid accidents. Therefore, we need to analyze the sub-actions that have different purposes in this phase.

Based on the definition of "pre-cutting action," this paper proposes a framework for analyzing mowing behaviors based on HHT action decomposition and realizes an empirical decomposition of pre-cutting action based on slope mowing data captured by a high-precision multi-sensor motion capture instrument. Then, based on the combination of relevant videos and interviews, this paper compares the differences between workers' similar sub-actions and investigates the effect of the change of the workers' joint angles on their stability in different sub-actions.

2. Related Studies and Hypotheses

2.1. Human Movement Analysis

In order to solve the problems caused by human behaviors, such as driving accidents or operational accidents, many studies have used motion capture devices to obtain and analyze human movements. For example, in our previous work, we collected and analyzed pre-braking action data from drivers with different driving experience by using a motion capture device to identify the influencing factors affecting driver behavior through a comparative analysis [7]. Moreover, there are two main branches in existing motion capture, camera and image analysis-based motion capture and wearable accelerometer-based motion capture, which have their own advantages and disadvantages.

There are many optional tools for motion capture based on camera and image processing technology, such as the recently popular MediaPipe from Google [17]. For example, Zhang et al. used YOLOv5 in MediaPipe and proposed a method for detecting deep

squatting movements by subjects' trunk angle, hip angle, and knee angle [18]. Similarly, according to the use of a camera and MediaPipe to track users' hand, head, and body movements, Ma et al. proposed a martial art posture recognition system [19].

On the other hand, many studies have used more accurate wearable accelerometers to capture human movements. Although not as convenient as camera-based motion capture, the higher accuracy gives researchers a wider scope for research. For example, Cockcroft et al. analyzed 10 bike riders' body movements via the data collected from the motion capture device called IMS. They validated the possibility of obtaining accurate outdoor exercise data from bicycles [20]. Moreover, Wouda et al. experimented with running movements by comparing the differences between three different motion capture devices. The devices they used are the Xsens MVN (which is also used in this research), Plug-In Gait, and OpenSim Gait2392 [21].

2.2. Hilbert–Huang Transform

Motion capture data are difficult to analyze due to their non-stationary and non-linear properties. These motion capture data are usually collected as a multivariate signal from the complicated human body structure by putting sensors on important joints of the body in the time series. Meanwhile, HHT has shown higher performance in analyzing non-stationary and non-linear signals than FT and wavelet transform. Based on the advantage of HHT, Dong et al. [12] presented a non-linear motion analysis framework using HHT, enabling researchers to non-linearly investigate human movements in the frequency domain. The previous study showed that human movements could be decomposed into a number of distinct motion primitives, ranging from high-frequency to low-frequency components. Moreover, this method also showed that HHT could help to generate training data in deep learning-based motion methods, such as humanoid robot motion design [13,14].

In total, as shown in these previous studies, human movements could be investigated in the frequency domain after decomposing motion data into motion primitives. However, in the previous research, the motion primitives were not discussed based on a behavioral view. Therefore, in this paper, to analyze the mowing motion of workers on slopes, we perform a more in-depth motion analysis of the auxiliary movements using HHT and discuss the results based on statistical methodologies.

3. Methodology

3.1. Definition: Mowing Motion on Slopes and Pre-Cutting Actions

To avoid confusion, the "pre-cutting" behaviors in this research is defined as the actions exhibited by a mowing worker's body before he/she releases kinetic energy to "cut the grass" by a mower (trimmer machine) during a whole mowing action.

As shown in Figure 1, pictures (1) to (7) are the key point slices of successive mowing actions on the same timeline. The pictures of (1) and (7) are almost identical, so (1) through (7) can be considered as a cycle of standard mowing movements. Therefore, based on the purpose of action, the entire mowing actions of the mowing worker's body can basically be divided into two stages: (1–4) lifting the mower to save kinetic energy and (5–7) swinging the mower to release kinetic energy. In contrast to our previous focus [15,16], in this study, we will focus on the actions of the "pre-cutting" part for analysis.

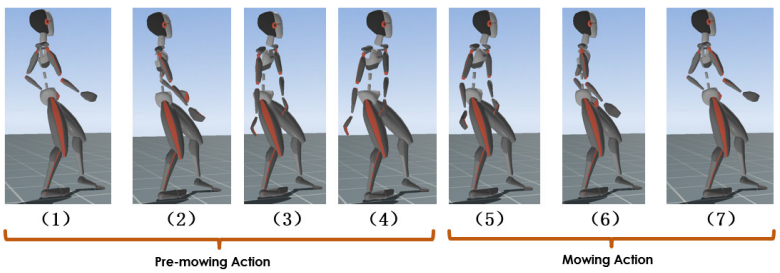

Figure 1. The Pre-cutting Behaviors in this Study.

3.2. Device: Body Motion Capture MVN

As shown in Figure 2, in order to obtain more precise data on the physical movements of the mowing work, a wearable device, Xsens MVN, is used that can collect body joints' 3D coordinates with high precision (60 Hz). Unlike traditional camera-based indoor devices, this device can provide extended outdoor experimental support.

Figure 2. Subject equipped with the motion capture device Xsens MVN.

A total of 23 joints can be collected by this device, MVN, including the spinal segments T12, T8, and tiptoe, which may not be considered in similar motion capture devices.

3.3. Method: Hilbert–Huang Transform

This section describes the HHT adopted in our proposed analysis framework. Although the mowing motion is more complex than normal human motion, most research has been limited to analysis in the time series. In contrast, a frequency-domain analysis method that accounts for periodicity is desirable because of the overlapping mowing motions. This study proposes a frequency-domain analysis method for the mowing motion using HHT since this method is suitable for human movements. Based on the analysis results, we discuss the relationship between the mowing motion and the decomposed motion primitives.

3.3.1. Hilbert–Huang Transform

The Hilbert–Huang Transform (HHT) involves two key steps to analyze signals [22]. First, the original signal is subjected to Empirical Mode Decomposition (EMD) to decompose the signal into a few intrinsic mode functions (IMFs). Second, the Hilbert Transform (HT) is applied to each IMF to yield the imaginary part of the IMF. That is, HT converts a non-linear monochromatic wave signal $A(t)\cos(\omega(t)t)$ into its imaginary part. This allows us to determine the instantaneous amplitude $A(t)$ and frequency $\omega(t)$ of the signal at each point in time. The key benefit of HHT is that it provides the instantaneous frequency of the monochromatic wave at each moment. Furthermore, numerous research efforts have

been made to expand EMD [23–25]. In addition, EMD has recently been reported to be very useful for creating motion data for deep learning [12,13].

As evident from the property of EMD, HHT distinguishes itself from FT. FT decomposes signals with linear oscillating components, while HHT decomposes them into a limited number of non-linear signals and underlying trends. HHT is deemed advantageous for analyzing non-linear and non-stationary mowing motions captured by multi-channel data.

Based on the above, this study focuses on the multi-channel data of motion-captured mowing motion. We apply HHT to this data and decompose the mowing motion into IMFs, which are the decomposed motion primitives during the mowing motion.

3.3.2. Empirical Mode Decomposition

HHT first adopts EMD that decomposes $x(t)$ into a finite number of IMFs $\sum_{k=1}^{n} \mathrm{IMF}_k^{\mathrm{Re}}(t)$ with one residual $r(t)$, as shown in (1) [22]. Next, the decomposed $\mathrm{IMF}_k^{\mathrm{Re}}$ is used as the real part, and the corresponding imaginary part $\mathrm{IMF}_k^{\mathrm{Im}}$ is obtained by HT to calculate the frequency $\omega(t)$ and amplitude $A(t)$ of $x(t)$ [26].

$$x(t) = \sum_{k-1}^{n} \mathrm{IMF}_k^{\mathrm{Re}}(t) + r(t) \tag{1}$$

The following criteria are the definition of IMFs:

- The difference between the local extrema and zero crossings should not exceed one.
- The mean value of the upper and lower envelopes derived from the local extrema should equal zero.

The EMD procedure decomposes $x(t)$ heuristically, as shown in the steps below.

1. Compute the residuals. (Initially, $r(t) = x(t)$).

$$r(t) = x(t) - \sum_{k=1}^{n} \mathrm{IMF}_k^{\mathrm{Re}}(t) \tag{2}$$

2. Initialize $\mathrm{IMF}_{\mathrm{old}}(t) = r(t)$ and retrieve $\mathrm{IMF}_k^{\mathrm{Re}}$.
   (a) The envelope $u(t)$ connecting the maxima of $\mathrm{IMF}_{\mathrm{old}}(t)$ and the envelope $l(t)$ connecting the minima are obtained by cubic spline interpolation, and the average of $u(t)$ and $l(t)$ is subtracted from $\mathrm{IMF}_{\mathrm{old}}(t)$.

$$\mathrm{IMF}_{\mathrm{new}}(t) = \mathrm{IMF}_{\mathrm{old}}(t) - \frac{u(t) + l(t)}{2} \tag{3}$$

   (b) If $\mathrm{IMF}_{\mathrm{new}}(t)$ satisfies the convergence condition ($\mathrm{SD} \leq \varepsilon$), it is added to the IMF set, $\sum_{k-1}^{n} \mathrm{IMF}_k^{\mathrm{Re}}(t)$. Otherwise, steps (a) and (b) are repeated.

$$\mathrm{SD} = \sum_{t=1}^{n} \frac{\left(\mathrm{IMF}_{\mathrm{old}}(t) - \mathrm{IMF}_{\mathrm{new}}(t)\right)^2}{\mathrm{IMF}_{\mathrm{new}}(t)^2} \tag{4}$$

3. Repeat steps 1 and 2 until all IMFs are extracted.

As we can see from the EMD algorithm, while FT and the wavelet transform assume a basis, such as a sin function, which transforms the signal into the frequency domain, EMD decomposes the signal sequentially using the above procedure, without assuming a basis, and terminates the loop at a threshold value. As a result, the principal components are extracted as oscillations, making them suitable for analyzing and editing real-world signal waveforms with complex noise.

3.3.3. Multivariate Empirical Mode Decomposition

EMD itself is an empirical decomposition and does not always accurately decompose signals into monochromatic waves. It is known that decomposition accuracy can be empirically improved by decomposing as multivariate data. For example, multivariate EMD (MEMD) extended to multiple channels has been proposed [25]. This study employs MEMD because human motion is sampled from multiple sensors simultaneously.

Next, we process the decomposed IMFs of mowing motions according to the previous study [27]. For all decomposed IMFs, the imaginary part $\mathrm{IMF}_k^{\mathrm{Im}}$ is obtained from $\mathrm{IMF}_k^{\mathrm{Re}}$ by HT. The frequency $\omega(t)$ and amplitude $A(t)$ are obtained. Weighted average frequencies and amplitudes of the decomposed IMFs can be used to analyze the biomechanical properties that is the speeds and movement ranges of each decomposed motion primitive. The motion analysis method using MEMD shows excellent performance in mowing motion analysis. Therefore, this study decomposes the mowing motion data recorded by multiple sensors into multiple channels using MEMD and analyzes them statistically for the joints that are considered major from the biomechanical view.

3.3.4. Joint Structure

Node graph architecture is widely adopted in different areas, such as social media network research [28,29]. On the other hand, motion data are captured using multiple sensors. Therefore, the data are usually mapped into a skeleton to calculate the joint rotation angle. Because of its multiple joints, the human body has also been considered as multiple nodes connected to each other [30]. Thus, in this research, we also calculate the body joint angles by considering the leg as a connected node structure.

As Figure 3 shows, the skeletal structure used in this study is rooted at the waist, and movement is described by 23 joints throughout the entire body. Each joint moves with three degrees of freedom: θ_x, θ_y, and θ_z. During the mowing motion, each motion primitive is a simple motion, and the body joints involved in this motion move at an arbitrary angle. Thus, if one motion primitive is to be captured, it is sufficient to take the MEMD of a specific angle and look at the instantaneous frequency. Therefore, because different joint angles are used in each swing, it is necessary to decompose the entire movement into three degrees of freedom, θ_x, θ_y, and θ_z, and calculate the Euclidean metric of the amplitude of each angle.

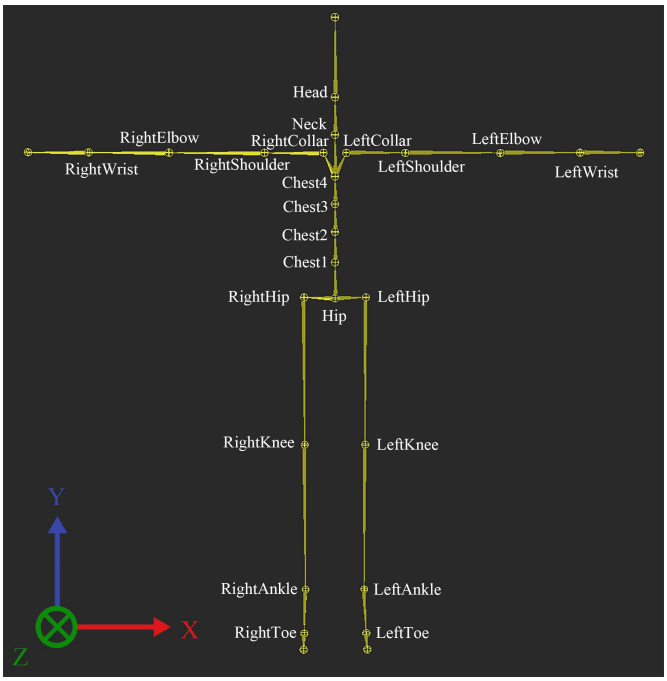

Figure 3. The Joint Structure of the Mowing Motion Skeleton.

3.3.5. Mowing Motion Decomposition

MEMD is used to extract motion primitives. Motion primitives are the most basic motion units in motion analysis and automatic generation. Many studies based on motion primitives have been conducted [31]. When considering the decomposed motion, confirmation by motion video is desirable. Each IMF, trend, and posture of mowing motion obtained from MEMD is written in Biovision Hierarchy (BVH) format, which describes the human body as a hierarchical skeletal model. However, in IMF motion analysis, the trend (residual), which is the time variation of the basic posture of mowing motion, must be added to reconstruct the motion. As Figure 4 shows, when decomposing the signal in MEMD, all joints and their 3-axis angles are empirically decomposed.

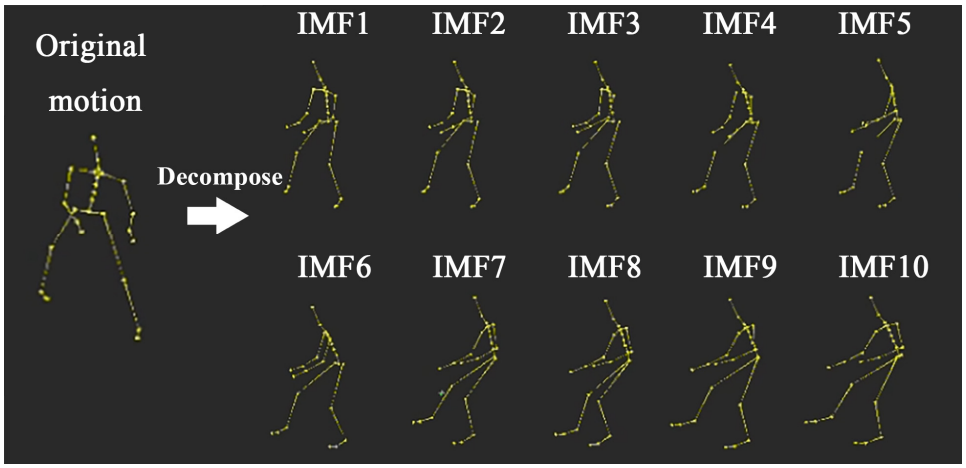

Figure 4. An Example of the Mowing Motion Decomposition.

Figure 4 demonstrates an instance of motion decomposition applied to the mowing motion. It shows that the original motion was decomposed into 10 IMFs. After adding the basic posture to each IMF, the motion primitives are obtained. By visualizing these extracted motion primitives of the mowing motion, we can see that IMF4 is the fast pre-cutting, and IMF5 is the slow pre-cutting. Because the cutting types might differ from the samples, we classified the type of samples based on evaluations of the decomposed motion primitives (BVHs shown in Figure 4) and the averaged frequencies of them. The details of this issue will be discussed in Section 5.

3.3.6. Average Amplitude and Frequency

Boashsah's work has shown that if the instantaneous frequency changes sufficiently slowly [32], then the instantaneous frequency obtained by applying an HT to the EMD-decomposed IMF can be smoothed. This property has been exploited by Niu et al., and they proposed the weighted average frequency algorithm (WAFA) [33]. Furthermore, recent research has shown that using WAFA to obtain each IMF's average amplitudes and frequencies could help researchers understand the physical meaning of these decomposed periodic modes [34].

The mowing motion analysis assumed in this paper calculated the average frequencies of all IMFs in the WAFA of the mowing motion. When the noise level of the mowing motion data was high, it was resolved as a non-linear wave $A(t)\cos(\omega(t)t)$ in a periodic or a cyclic multidimensional sphere. A series of mowing motions was decomposed into a single non-linear monochromatic wave (IMF). In this case, for each IMF, the amplitude $A(t)$ of that mode had almost zero amplitude at the time when there is no motion. When averaging in instantaneous frequencies to obtain the averaged frequency, it is necessary to multiply $A(t)$ by $\omega(t)$. This algorithm also obtains the average frequency for each IMF described below. For the average amplitude, the arithmetic mean was adopted in this study.

3.4. Model: Joint Angular Calculation-based Body Movement Analysis

According to the assumption that "the vast majority of single-purpose active actions can be decomposed into different sub-actions" and given our previous research experience [15,16], we tried to propose a joint angle calculation-based comparative model for normal body movement analysis. As shown in Figure 5, for general motion capture experiments, the model has three main components: field experiments, data processing, and body movement analysis.

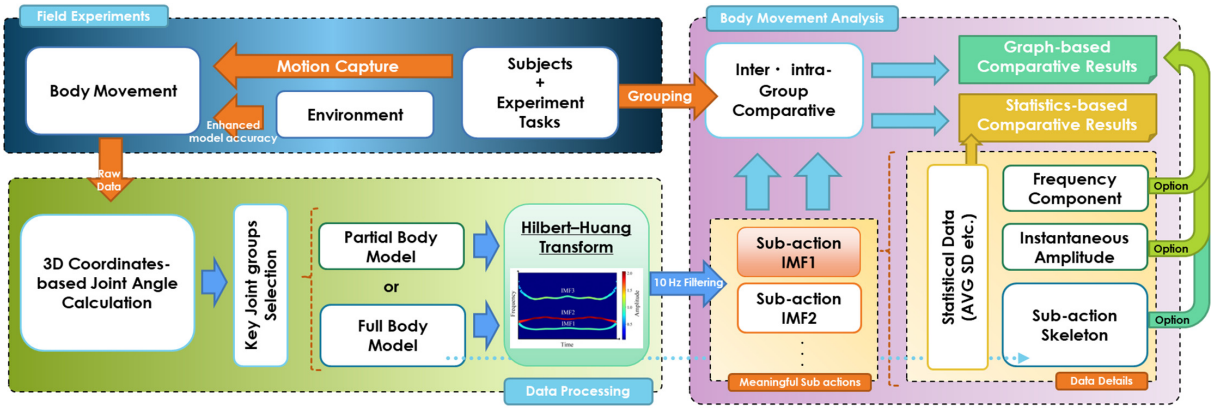

Figure 5. Joint Angular Calculation-based Body Movement Analysis Model.

- Field experiments: The purpose of the vast majority of human behavior comparison experiments is to find out the similarities and differences between different subject groups. Therefore, this model argues that in the field experiment stage, it is necessary to group subjects in advance for the purpose of the experiment and to collect the environmental data of the experimental site as objectively as possible. This will enhance the 3D model accuracy captured by the devices for the final human body movements.
- Data processing: After receiving the raw data of body movements, this model does not put the data into machine learning or other black-box algorithms directly. Instead, the model calculates all the joint angles of the subject's body based on their original 3D coordinates before the analysis and then selects the most relevant parts to represent their body movement characteristics data for calculation according to the experimental purpose. Based on this, the corresponding model (full or partial) will be selected, and the HHT movement decomposition method will be used to decompose the target body movements to obtain the raw overall statistics and time-series-based graphical data for the following analysis.
- Body movement analysis: Because not all sub-actions have an obvious purpose, some minor redundant actions that are not even perceptible to humans need to be eliminated before the analysis (10 Hz filtering). In combination with the previous grouping of subjects, the model classifies all meaningful sub-actions (IMF1, IMF2,...) of the relevant data into two types (statistic data and graph data) before the between and within groups comparative analyses. Different types of sub-action data can be analyzed in different comparative ways. This will facilitate model users' interpretation and discussion of the purpose and effect of the target sub-action from different perspectives of the whole and time series.

4. Field Experiments and Dataset

4.1. Field Experiments

A set of experiments was conducted at Kouchi, Higashi Hiroshima, Hiroshima, Japan. A conventional U-shaped portable mower was used for the experiments. This type of mower allows the worker to hold it in both hands and mow in a prescribed direction (from left to right).

As shown in Figure 6, the sloping area has a slope angle of greater than or equal to 30 degrees, and the trigonometric tangent is expressed as a percentage of 30 degrees = 57%. The weeds are thick and have small stones hidden in them, which increases the difficulty of manual mowing and the risk of falling during the operation. All mowing workers needed to make several horizontal trips to complete the work in the area they were responsible for. (The slope height is about 10 m). All subject workers were asked to wear the motion capture suit and perform their usual mowing work. Workers' physical data was also collected before the experiments. Then, a post-test interview was conducted with each subject to identify details that could not be obtained through the device.

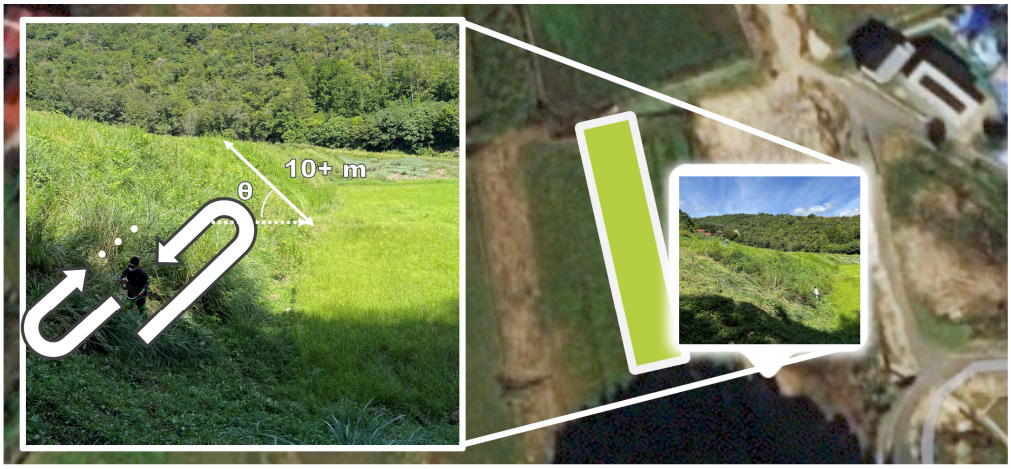

Figure 6. An Example of the Mowing Motion Decomposition.

As shown in Table 1, 5 experienced mowing workers, each with more than 5 years of experience in the area, were invited to participate in the experiment. All subjects participating in the experiment were right-handed, male, in good health, and had no cognitive impairment problems.

Table 1. Details of the Experimental Subjects.

No.	Body Height	Arm Span	Hip Height	Age	Experience
1	165	163	90	74	40 years~
2	165	161	97	66	40 years~
3	176	167	107	68	8 years~
4	163	170	90	46	6 years~
5	176	167	107	69	10 years~

4.2. Dataset

Eventually, 567 sets of data were collected. As mentioned above, we focused only on the pre-cutting behavior part for the analysis. Based on the pre-processing, we parsed the sub-action (IMFs) composition by the HHT decomposition method, which meant we could obtain data, including the mowing workers' movement trends, as well as the frequency and amplitude for all IMFs' body joints.

For the statistical analysis, the HHT decomposition method used in this paper divided each action according to frequency. However, according to a previous study [35], subjects would not be able to control movements with an action frequency of less than 10 Hz. This means that these movements can be considered as redundant actions and can be ignored.

Therefore, only IMFs no. 3, 4, and 5 were eligible (>10 Hz) in our research, and the measures for each IMF were used for comparative analysis. As shown in Table 2, we considered a total of 23 groups of human joints in terms of their angles and their variations, as follows.

Table 2. Calculated Measures.

No.	Measure	Abbreviations	No.	Measure	Abb.
1	Hip	Hip	12	Right Toe	Rtoe
2	Chest1-4	Chest1-4	13	Left Collar	Lcollar
3	Neck	Neck	14	Left Shoulder	Lshoulder
4	Head	Head	15	Left Elbow	Lelbow
5	Right Collar	Rcollar	16	Left Wrist	Lwrist
6	Right Shoulder	Rshoulder	17	Left Hip	Lhip
7	Right Elbow	Relbow	18	Left Knee	Lknee
8	Right Wrist	Rwrist	19	Left Ankle	Lankle
9	Right Hip	Rhip	20	Left Toe	Ltoe
10	Right Knee	Rknee	21		
11	Right Ankle	Rankle	22		

In addition, according to the characteristics of the mowing movement, we used all joint data for the global analysis. This allowed us to obtain the skeletal data, which helped to identify the purpose of all sub-actions easily.

5. Data Processing and Analysis

To confirm the purpose of the different sub-actions, we compared pre-cutting actions between different mowing workers and examined the effect of whole-body joint changes on mowing stability.

5.1. HHT-based Actions Decomposition and Classification

In this study, we decomposed motion capture data into several IMFs from high frequency to low frequency by putting all the joint angles into MEMD. Table 3 shows the average frequencies of each decomposed IMF obtained from six samples.

Table 3. Average Frequencies of Each Decomposed IMF.

	S1	S2	S3	S4	S5	S6
IMF 1	3.023	4.683	4.589	3.325	3.718	2.097
IMF 2	2.871	3.375	2.979	2.122	2.217	2.035
IMF 3	1.852	2.040	1.833	1.55	1.249	2.078
IMF 4	1.035	1.158	0.999	0.900	0.707	1.511
IMF 5	0.613	0.703	0.574	0.517	0.442	0.959
IMF 6	0.355	0.436	0.371	0.28	0.247	0.601
IMF 7	0.178	0.242	0.190	0.153	0.139	0.347
IMF 8	0.097	0.133	0.100	0.080	0.072	0.191
IMF 9	0.052	0.069	0.057	0.044	0.038	0.104
IMF 10	0.031	0.038	0.031	0.022	0.024	0.056

By analyzing the decomposed IMFs, we observed that two different cutting actions could be extracted from the original motion data: (a) Fast pre-cutting is performed at about 1.1 s–2.5 s (0.4 Hz–0.9 Hz), corresponding to IMF4–6. (b) Slow pre-cutting is performed at about 5 s–2 s (0.2 Hz–0.5 Hz), corresponding to IMF5–7. Underlined numbers in Table 4 show the fast pre-cutting and slow pre-cutting decomposed as different values and different motion speeds (frequency) caused by variations in the cutting styles of each person.

Table 4. Results for Different Mowing Experience (Freq. Fast).

Measure	Mowing Experience	N	Mean Rank	U	W	Z	*p*	Effect Size
Hip_freq *	Novice	43	49.19	293	888	−4.49	0.00	−0.51225
	Experienced	34	26.12					
Chest_freq *	Novice	43	49.47	281	876	−4.62	0.00	−0.52642
	Experienced	34	25.76					
Chest2_freq *	Novice	43	48.93	304	899	−4.38	0.00	−0.49915
	Experienced	34	26.44					
Chest3_freq	Novice	43	49.26	290	885	−4.52	0.00	−0.51556
	Experienced	34	26.03					
Chest4_freq *	Novice	43	49.44	282	877	−4.61	0.00	−0.52492
	Experienced	34	25.79					
Neck_freq *	Novice	43	47.93	347	942	−3.94	0.00	−0.4489
	Experienced	34	27.71					
Head_freq *	Novice	43	49.77	268	863	−4.75	0.00	−0.54131
	Experienced	34	25.38					
Rcollar_freq *	Novice	43	47.23	377	972	−3.63	0.00	−0.4138
	Experienced	34	28.59					
Rshoulder_freq *	Novice	43	46.21	421	1016	−3.18	0.00	−0.36239
	Experienced	34	29.88					
Relbow_freq *	Novice	43	46.98	388	983	−3.52	0.00	−0.41273
	Experienced	34	28.91					
Rwrist_freq *	Novice	43	45.37	457	1052	−2.81	0.01	−0.32343
	Experienced	34	30.94					
Lcollar_freq *	Novice	43	46.37	414	1009	−3.25	0.00	−0.376
	Experienced	34	29.68					
Lshoulder_freq *	Novice	43	44.33	502	1097	−2.35	0.02	−0.26769
	Experienced	34	32.26					
Lelbow_freq *	Novice	43	47.65	359	954	−3.82	0.00	−0.43487
	Experienced	34	28.06					
Lwrist_freq *	Novice	43	45.91	434	1029	−3.05	0.00	−0.34724
	Experienced	34	30.26					
Rhip_freq *	Novice	43	44.60	490	1085	−2.47	0.01	−0.28172
	Experienced	34	31.91					
Rknee_freq *	Novice	43	51.42	197	792	−5.48	0.00	−0.62428
	Experienced	34	23.29					
Rankle_freq *	Novice	43	46.49	409	1004	−3.30	0.00	−0.37641
	Experienced	34	29.53					
Rtoe_freq ‡	Novice	43	42.88	564	1159	−1.71	0.09	−0.19521
	Experienced	34	34.09					
Lhip_freq *	Novice	43	47.53	364	959	−3.77	0.00	−0.42962
	Experienced	34	28.21					
Lknee_freq *	Novice	43	47.26	376	971	−3.64	0.00	−0.41544
	Experienced	34	28.56					
Lankle_freq *	Novice	43	47.79	353	948	−3.88	0.00	−0.44194
	Experienced	34	27.88					
Ltoe_freq *	Novice	43	45.05	471	1066	−2.67	0.01	−0.33933
	Experienced	34	31.35					

‡ $p < 0.1$, * $p < 0.05$.

Because all joint data had been inputted into MEMD to achieve multivariate decomposed IMFs, we could visualize the decomposed motion by mapping the IMFs to the original skeleton. As shown in Figure 7, these two different cutting actions can be clearly classified.

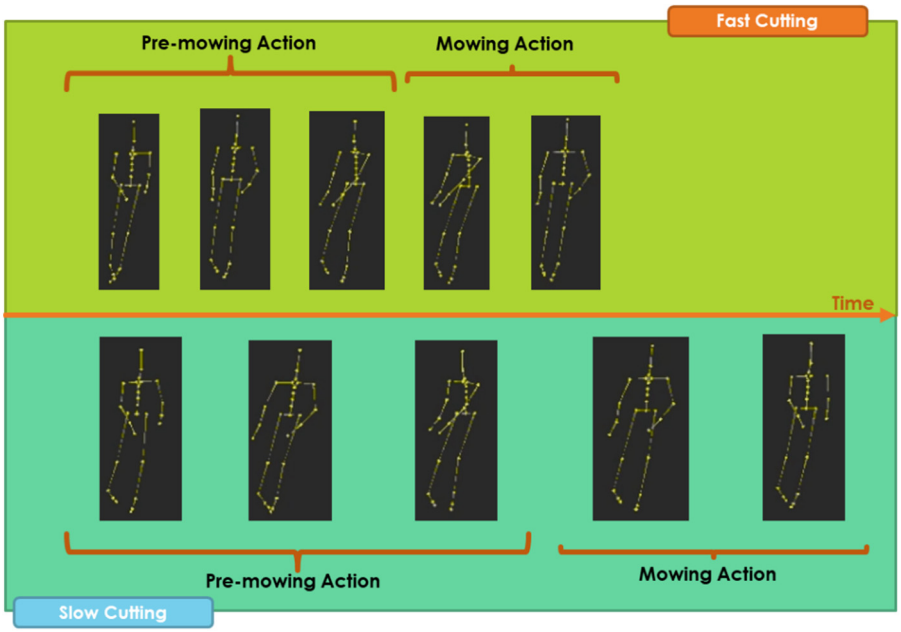

Figure 7. Two Different Types of Cutting Actions (Fast/Slow).

Therefore, by investigating both different cuttings of each sample, our research can reveal the difference between beginners and experts, thus helping beginners to improve their skill of grass cutting. Our results can also provide the features as training data for risk of falling detection using deep learning by investigating the pre-cutting movements of the two extracted motion types.

5.2. Differences between Workers with Different Mowing Experience

We included a less experienced subject in our latest slope mowing experiment. Therefore, we could discover the difference in movements resulting from different mowing experience. Based on the two different pre-cutting actions (fast/slow) that we decomposed using the HHT method, the data (fast/slow pre-cutting action's frequency and amplitude) were analyzed using a non-parametric identification method, namely the independent-samples Mann–Whitney U test. In addition, more data were collected for subject number 5 than for the other subjects. Therefore, his data were not included in this section to avoid any bias.

5.2.1. Differences between Workers with Different Mowing Experience (Fast)

Based on the Kolmogorov Smirnov normality test and related Levene's test, we find that the data we collected did not conform to a normal distribution but generally consistent with assumption of homogeneity of variance. The independent-samples Mann–Whitney U test can be used in this case.

As shown in Table 4, for the "fast pre-cutting" action's frequency, the results showed that the experienced workers differed significantly from novices in almost all metrics. In contrast, for the "fast pre-cutting" action's amplitude, shown in Table 5, most of the indicators did not show significant differences, whereas the differences were mainly concentrated in the indicators of Rshoulder_amp, Relbow_amp, Rwrist_amp, and Lshoulder_amp.

Table 5. Results for Different Mowing Experience (Amp. Fast).

Measure	Mowing Experience	N	Mean Rank	U	W	Z	*p*	Effect Size
Hip_amp	Novice	43	37.47	665	1611	−0.68	0.50	−0.077
	Experienced	34	40.94					
Chest_amp	Novice	43	36.95	643	1589	−0.90	0.37	−0.103
	Experienced	34	41.59					
Chest2_amp	Novice	43	37.44	664	1610	−0.69	0.49	−0.078
	Experienced	34	40.97					
Chest3_amp	Novice	43	37.16	652	1598	−0.81	0.42	−0.092
	Experienced	34	41.32					
Chest4_amp	Novice	43	36.88	640	1586	−0.93	0.35	−0.106
	Experienced	34	41.68					
Neck_amp	Novice	43	38.95	729	1675	−0.02	0.98	−0.002
	Experienced	34	39.06					
Head_amp	Novice	43	39.88	693	1288	−0.39	0.70	−0.044
	Experienced	34	37.88					
Rcollar_amp	Novice	43	38.26	699	1645	−0.33	0.74	−0.037
	Experienced	34	39.94					
Rshoulder_amp *	Novice	43	34.28	528	1474	−2.08	0.04	−0.237
	Experienced	34	44.97					
Relbow_amp *	Novice	43	28.56	282	1228	−4.61	0.00	−0.525
	Experienced	34	52.21					
Rwrist_amp *	Novice	43	29.63	328	1274	−4.13	0.00	−0.471
	Experienced	34	50.85					
Lcollar_amp	Novice	43	42.40	585	1180	−1.50	0.13	−0.171
	Experienced	34	34.71					
Lshoulder_amp *	Novice	43	34.53	539	1485	−1.97	0.05	−0.224
	Experienced	34	44.65					
Lelbow_amp	Novice	43	35.26	570	1516	−1.65	0.10	−0.188
	Experienced	34	43.74					
Lwrist_amp ‡	Novice	43	34.95	557	1503	−1.78	0.07	−0.203
	Experienced	34	44.12					
Rhip_amp	Novice	43	39.86	694	1289	−0.38	0.70	−0.043
	Experienced	34	37.91					
Rknee_amp	Novice	43	40.35	673	1268	−0.59	0.55	−0.068
	Experienced	34	37.29					
Rankle_amp	Novice	43	34.67	545	1491	−1.91	0.06	−0.217
	Experienced	34	44.47					
Rtoe_amp	Novice	43	35.95	600	1546	−1.34	0.18	−0.153
	Experienced	34	42.85					
Lhip_amp	Novice	43	38.58	713	1659	−0.18	0.85	−0.021
	Experienced	34	39.53					
Lknee_amp	Novice	43	35.47	579	1525	−1.56	0.12	−0.178
	Experienced	34	43.47					
Hip_amp	Novice	43	41.65	617	1212	−1.17	0.24	−0.133
	Experienced	34	35.65					
Chest_amp	Novice	43	38.14	694	1640	−0.38	0.70	−0.043
	Experienced	34	40.09					

‡ $p < 0.1$, * $p < 0.05$.

This suggests that differences in mowing experience on slopes mainly affect the speed of mowing workers' whole-body movements and have a limited effect on the overall force used. As special cases, experienced workers concentrated a higher force in the right arm (shoulder, elbow, and wrist) and left shoulder (all subjects were right-handed) to increase the efficiency of mowing.

5.2.2. Differences between Workers with Different Mowing Experience (Slow)

The same analysis was performed for the slow pre-cutting action's frequency and amplitude. However, the results were more complicated. As shown in Table 6, for the "slow pre-cutting" action's frequency, most of the indicators did not show significant differences, whereas the differences were mainly concentrated in the indicators of Chest_freq, Chest3_freq, and Chest4_freq. In contrast, for the "slow pre-cutting" action's amplitude, shown in Table 7, the experienced workers differed significantly from novices in only the metrics of Chest_amp, Chest2_amp, Chest3_amp, Chest4_amp, Rshoulder_amp, Relbow_amp, Rwrist_amp, Lcollar_amp, Lshoulder_amp, Lwrist_amp, and Rankle_amp.

Table 6. Results for Different Mowing Experience (Freq. Slow).

Measure	Mowing Experience	N	Mean Rank	U	W	Z	*p*	Effect Size
Hip_freq	Novice	43	37.86	682	1628	−0.50	0.62	−0.05728
	Experienced	34	40.44					
Chest_freq *	Novice	43	44.07	513	1108	−2.24	0.03	−0.25485
	Experienced	34	32.59					
Chest2_freq	Novice	43	44.12	511	1106	−2.26	0.02	−0.25719
	Experienced	34	32.53					
Chest3_freq *	Novice	43	43.63	532	1127	−2.04	0.04	−0.23264
	Experienced	34	33.15					
Chest4_freq *	Novice	43	43.58	534	1129	−2.02	0.04	−0.2303
	Experienced	34	33.21					
Neck_freq	Novice	43	42.07	599	1194	−1.35	0.18	−0.15431
	Experienced	34	35.12					
Head_freq	Novice	43	43.02	558	1153	−1.77	0.08	−0.20224
	Experienced	34	33.91					
Rcollar_freq	Novice	43	40.98	646	1241	−0.87	0.38	−0.09937
	Experienced	34	36.50					
Rshoulder_freq	Novice	43	37.77	678	1624	−0.54	0.59	−0.06196
	Experienced	34	40.56					
Relbow_freq	Novice	43	42.47	582	1177	−1.53	0.13	−0.17418
	Experienced	34	34.62					
Rwrist_freq	Novice	43	41.60	619	1214	−1.15	0.25	−0.13093
	Experienced	34	35.71					
Lcollar_freq	Novice	43	42.23	592	1187	−1.43	0.15	−0.16249
	Experienced	34	34.91					
Lshoulder_freq	Novice	43	41.91	606	1201	−1.28	0.20	−0.14613
	Experienced	34	35.32					

Table 6. *Cont.*

Measure	Mowing Experience	N	Mean Rank	U	W	Z	*p*	Effect Size
Lelbow_freq ‡	Novice	43	43.33	545	1140	−1.91	0.06	−0.21744
	Experienced	34	33.53					
Lwrist_freq ‡	Novice	43	43.16	552	1147	−1.84	0.07	−0.20926
	Experienced	34	33.74					
Rhip_freq	Novice	43	41.19	637	1232	−0.96	0.33	−0.10989
	Experienced	34	36.24					
Rknee_freq	Novice	43	42.60	576	1171	−1.59	0.11	−0.1812
	Experienced	34	34.44					
Rankle_freq	Novice	43	42.65	574	1169	−1.61	0.11	−0.18354
	Experienced	34	34.38					
Rtoe_freq	Novice	43	38.49	709	1655	−0.23	0.82	−0.02572
	Experienced	34	39.65					
Lhip_freq	Novice	43	41.81	610	1205	−1.24	0.21	−0.14145
	Experienced	34	35.44					
Lknee_freq	Novice	43	40.67	659	1254	−0.74	0.46	−0.08417
	Experienced	34	36.88					
Lankle_freq	Novice	43	40.19	680	1275	−0.52	0.60	−0.05962
	Experienced	34	37.50					
Ltoe_freq	Novice	43	40.40	671	1266	−0.62	0.54	−0.07014
	Experienced	34	37.24					

‡ $p < 0.1$, * $p < 0.05$.

Table 7. Results for Different Mowing Experience (Amp. Slow).

Measure	Mowing Experience	N	Mean Rank	U	W	Z	*p*	Effect Size
Hip_amp	Novice	43	35.70	589	1535	−1.46	0.15	-0.166
	Experienced	34	43.18					
Chest_amp *	Novice	43	34.28	528	1474	−2.08	0.04	−0.23731
	Experienced	34	44.97					
Chest2_amp *	Novice	43	34.77	549	1495	−1.87	0.06	−0.21276
	Experienced	34	44.35					
Chest3_amp *	Novice	43	34.35	531	1477	−2.05	0.04	−0.23381
	Experienced	34	44.88					
Chest4_amp *	Novice	43	34.14	522	1468	−2.14	0.03	−0.24433
	Experienced	34	45.15					
Neck_amp	Novice	43	36.65	630	1576	−1.04	0.30	−0.11807
	Experienced	34	41.97					
Head_amp	Novice	43	37.00	645	1591	−0.88	0.38	−0.10054
	Experienced	34	41.53					
Rcollar_amp	Novice	43	38.47	708	1654	−0.24	0.81	−0.02689
	Experienced	34	39.68					

Table 7. *Cont.*

Measure	Mowing Experience	N	Mean Rank	U	W	Z	*p*	Effect Size
Rshoulder_amp *	Novice	43	30.84	380	1326	−3.60	0.00	−0.41033
	Experienced	34	49.32					
Relbow_amp *	Novice	43	24.19	94	1040	−6.53	0.00	−0.74467
	Experienced	34	57.74					
Rwrist_amp *	Novice	43	26.93	212	1158	−5.32	0.00	−0.60672
	Experienced	34	54.26					
Lcollar_amp *	Novice	43	47.40	370	965	−3.70	0.00	−0.42202
	Experienced	34	28.38					
Lshoulder_amp *	Novice	43	33.37	489	1435	−2.48	0.01	−0.2829
	Experienced	34	46.12					
Lelbow_amp	Novice	43	38.00	688	1634	−0.44	0.66	−0.05027
	Experienced	34	40.26					
Lwrist_amp *	Novice	43	32.56	454	1400	−2.84	0.00	−0.32382
	Experienced	34	47.15					
Rhip_amp	Novice	43	41.23	635	1230	−0.98	0.32	−0.11223
	Experienced	34	36.18					
Rknee_amp	Novice	43	41.09	641	1236	−0.92	0.36	−0.10521
	Experienced	34	36.35					
Rankle_amp *	Novice	43	34.33	530	1476	−2.06	0.04	−0.23497
	Experienced	34	44.91					
Rtoe_amp	Novice	43	36.05	604	1550	−1.30	0.19	−0.14847
	Experienced	34	42.74					
Lhip_amp	Novice	43	36.65	630	1576	−1.04	0.30	−0.11807
	Experienced	34	41.97					
Lknee_amp	Novice	43	36.33	616	1562	−1.18	0.24	−0.13444
	Experienced	34	42.38					
Lankle_amp	Novice	43	40.47	668	1263	−0.65	0.52	−0.07365
	Experienced	34	37.15					
Ltoe_amp ‡	Novice	43	34.91	555	1501	−1.81	0.07	−0.20575
	Experienced	34	44.18					

‡ $p < 0.1$, * $p < 0.05$.

Such results suggest that, for most of the slow pre-cutting action, the difference in speed between workers with different mowing experience was not significant, but rather the difference in the force used was more pronounced. This difference was mainly in the right arm (shoulder, elbow, and wrist) and left arm (shoulder and wrist). Thus, experienced workers in the slow pre-cutting action had a similar speed as novices but had more power in their hand movements. Together with the results for fast pre-cutting, this indicates that experienced workers are more confident in using force compared to novices.

In addition, the results for the partial spinal joints (chests) showed that experienced workers had less spinal flexion, but used more force during the preparatory mowing maneuver. One possible explanation is that experienced workers move more steadily, but use force more firmly, thus ensuring the quality of the mowing.

5.3. Falling Risk Analysis

This paper focuses only on the pre-cutting part of the whole mowing action. In our previous study [14], we discussed the influence of various joint movements on worker

stability in general mowing motion (cutting). Therefore, in this section, we will discuss the influence of changes in the angle of each joint and related body characteristics on the stability of workers in the pre-cutting movement to identify the safety postures that minimize the possibility of workers' falling risk.

Similar to our previous studies, which used the standard deviation of the waist joint angle to judge the risk of falling, this paper will comprehensively judge the risk of falling by taking the standard deviation of the corresponding hip joint angle of different sub-movements (fast/slow pre-cutting actions). Because the frequency and amplitude of each group of movements were respectively taken as indicators in this paper, we had four indicators that could be used as dependent variables to evaluate the impact of other movement joints on the risk of falling: SD_hip (Freq. Fast), SD_hip (Amp. Fast), SD_hip (Freq. Slow), and SD_hip (Amp. Slow).

After correlation pretreatment, we determined that the dependent variables mentioned above basically conformed to a normal distribution. Therefore, stepwise regression analysis is chosen to confirm the angle changes of each joint and the stability of the workers' relationship.

5.3.1. Falling Risk Analysis for Pre-Cutting SD_hip (Freq. Fast)

First, the stepwise regression method was used to calculate the influence of different joint angle changes on the dependent variable SD_hip (Freq. Fast). Because the original data of the dependent variable did not quite conform to a normal distribution, we analyzed it on the basis of logarithm (the adjusted data were close to a normal distribution).

The results (Table 8) showed that the most important factors affecting the fast pre-cutting action were the head (Head_amp and Head_freq) and left leg part (Lhip_freq, Lankle_freq, Ankle_height, and Foot_or_Shoe_length).

Table 8. Results of Stepwise Regression of SD_hip (Freq. Fast).

Measure	Unstandardized Coef.		Standardized Coef.	T	Sig.
	B	Std. Error	Beta		
(Constant)	4.220	1.760		2.398	0.017
Ankle_height	0.109	0.023	0.250	4.680	0.000
Lhip_freq	0.196	0.034	0.255	5.749	0.000
Head_amp	−0.021	0.005	−0.165	−3.834	0.000
Lankle_freq	0.140	0.046	0.140	3.014	0.003
Foot_or_Shoe_length	−0.239	0.062	−0.204	−3.854	0.000
Head_freq	0.108	0.040	0.121	2.714	0.007

$R = 0.599$, $R^2 = 0.359$, R^2 adjust = 0.349.

Specifically, the results showed that the faster the rate of change in the joints of a worker's head, the faster the frequency of vibrations in the worker's waist. One possible explanation is that to gather kinetic energy more efficiently, a worker's head acts as a stabilizing force in the fast pre-cutting action.

In addition, the results for the right leg indicated that the left leg was the power output source in the pre-cutting movement and that the faster the joint transformation speed, the higher the vibration frequency of the worker's waist. Therefore, workers may need to be careful not to overexert their left leg when performing the pre-cutting actions.

Moreover, another interesting result was that the decomposition indicated the effect of the workers' physical characteristics (Ankle_height and Foot_or_Shoe_length) on their stability. Workers with larger feet and lower ankles had fewer waist vibrations during movement. This may be explained by the steadiness of larger feet, as well as the lower center of gravity that may come with lower ankles.

5.3.2. Falling Risk Analysis for Pre-Cutting SD_hip (Amp. Fast)

Next, the stepwise regression method was also used to calculate the influence of different joint angle changes on the dependent variable SD_hip (Amp. Fast). Because the dependent variables basically conformed to a normal distribution, we used the original data for the analysis, and the results were as follows.

As shown in Table 9, the most important factors affecting the fast pre-cutting action were Body_height, chest2_amp, and the ankle part (Rankle_amp and Lankle_amp).

Table 9. Results of Stepwise Regression of SD_hip (Amp. Fast).

Measure	Unstandardized Coef.		Standardized Coef.	T	Sig.
	B	Std. Error	Beta		
(Constant)	−66.549	4.873		−13.658	0.000
Rankle_amp	0.389	0.041	0.324	9.551	0.000
Body_height	0.384	0.028	0.385	13.807	0.000
Chest2_amp	1.669	0.190	0.280	8.787	0.000
Lankle_amp	0.277	0.040	0.230	6.950	0.000

$R = 0.755$, $R^2 = 0.570$, R^2 adjust = 0.567.

In particular, a person's body height had a positive effect on the intensity of waist vibrations during pre-cutting, which could mean that taller people have a greater falling risk during mowing actions. One possibility is that a greater body height raises workers' center of gravity, which is not conducive to keeping the waist stable.

In addition, the ankle joint force also affected the vibration intensity of the waist, and the direction was positive. This was consistent with the results in Table 9, which can be interpreted as body shaking caused by the exertion of the ankle.

5.3.3. Falling Risk Analysis for Pre-Cutting SD_hip (Freq. Slow)

The same analysis was performed for the slow pre-cutting data to calculate the influence of different joint angle changes on the dependent variable SD_hip (Freq. Slow). Because the dependent variables basically conformed to a normal distribution, we used the original data for the analysis, and the results were as follows.

As shown in Table 10, the results showed that the most important factors affecting the slow pre-cutting action were Hip_height, Age, Neck_freq, and the left upper body part (Lcollar_freq and Lhip_freq) and ankle part (Rankle_amp and Lankle_amp).

Table 10. Results of Stepwise Regression of SD_hip (Freq. Slow).

Measure	Unstandardized Coef.		Standardized Coef.	T	Sig.
	B	Std. Error	Beta		
(Constant)	1.602	0.468		3.424	0.001
Rankle_freq	0.207	0.041	0.196	5.022	0.000
Lhip_freq	0.189	0.036	0.203	5.247	0.000
Neck_freq	0.147	0.042	0.135	3.541	0.000
Hip_height	−0.025	0.005	−0.215	−5.052	0.000
Lcollar_freq	0.150	0.039	0.141	3.835	0.000
Lankle_freq	0.138	0.043	0.128	3.235	0.001
Age	0.018	0.006	0.136	3.199	0.001

$R = 0.528$, $R^2 = 0.279$, R^2 adjust = 0.270.

Specifically, the role of the rate of joint change in the left and right ankle was significant in influencing the frequency of waist vibrations. The results show the effect of age on slow pre-cutting, with higher ages showing a faster frequency of waist vibrations, which is consistent with conventional predictions.

In addition, the workers' hip height was inversely proportional to the frequency of waist vibrations, meaning that a person with a higher hip height would be more stable during slow pre-cutting. One possible explanation is that a higher hip height can drive the knee in a powerful position to drive down and back [36], which allows workers to better maintain a stable posture.

5.3.4. Falling Risk Analysis for Pre-Cutting SD_hip (Amp. Slow)

Finally, the stepwise regression method was also used to calculate the influence of different joint angle changes on the dependent variable SD_hip (Amp. Slow). Because the dependent variables basically conformed to a normal distribution, we used the original data for the analysis, and the results were as follows.

As shown in Table 11, the results showed that the most important factors affecting the slow pre-cutting action were mowing experience (Exp), Lcollar_amp, Ltoe_amp, Rknee_amp, and the ankle part (Rankle_amp and Lankle_amp).

Table 11. Results of Stepwise Regression of SD_hip (Amp. Slow).

Measure	Unstandardized Coef.		Standardized Coef.	T	Sig.
	B	Std. Error	Beta		
(Constant)	0.430	0.318		1.352	0.177
Lankle_amp	0.999	0.048	0.653	20.909	0.000
Ltoe_amp	−0.516	0.064	−0.209	−8.022	0.000
Rankle_amp	0.312	0.046	0.218	6.852	0.000
Rknee_amp	−0.081	0.013	−0.161	−5.987	0.000
Lcollar_amp	0.577	0.118	0.134	4.877	0.000
Exp	−0.059	0.014	−0.113	−4.328	0.000

$R = 0.804$, $R^2 = 0.646$, R^2 adjust = 0.642.

In particular, the effect of the left and right ankles on the power of waist vibrations was significant, which is consistent with what we have learned so far. In addition, the impact of the left toe and the right knee were both negative, which may mean that the worker needs to exert as much force as possible on their left toe and right knee (bending the left toe and right knee to lift the mower) to maintain stability during slow pre-cutting.

6. Discussion & Conclusions

We proposed a joint angular calculation-based body movement analysis model using the HHT action decomposition method and analyzed data for the pre-cutting action of workers mowing on slopes. The aim of this paper was to analyze the main patterns (IMFs) in the pre-cutting actions, identify the differences in movements between workers with different mowing experience, and find the main factors affecting the falling risk (stability) of workers in these different patterns.

Specifically, the results of the HHT method showed that two main sub-actions were confirmed during mowing, which we named as fast pre-cutting and slow pre-cutting by their action speed. The results showed that for the fast pre-cutting action, experienced workers had higher scores than relatively less-experience (novice) workers in both whole-body speed and use of power in some key joints (right arm). In contrast, for the slow pre-cutting action, most of the differences were in the force used. We can surmise that experienced workers are more confident than novices in using additional force to remain cutting efficiently, while keeping their balance to avoid falling.

Moreover, the results of falling risk showed that some of workers' physical characteristics affected their degree of physical stability during pre-cutting actions. These characteristics were body height, hip height, ankle height, and foot or shoe length. In addition, while demonstrating that worker experience and age also influenced the results to some extent, the correlation results showed that for all cases, the worker's ankle joint angle variation was the most important influencing element. This means that during the different

sub-movements, more attention needs to be paid to ankle parts than to other parts of the body to prevent falls. The results obtained in this paper suggest that these influencing factors should be emphasized in the training of mowing workers and the development of auxiliary equipment, etc.

The study had some limitations. First, the number of workers engaged in mowing was relatively small, and most of them were old. Thus, the sample size discussed in this study was a bit small. Second, this is an exploratory study, and the results may not be taken as confirmatory.

In the future, we plan to collect eye movement data of workers in the grass-cutting experiment and analyze the relationship between eye movement, body movement, and stability through data fusion. The management of the ridges and slopes for paddy fields in mountainous areas requires more time and labor than the flat areas, so the cost is relatively high. The development of a mowing model that increases efficiency while ensuring safety will also lead to a reduction of mowing costs.

Author Contributions: Conceptualization, B.W. and R.D.; methodology, B.W. and R.D.; software, B.W. and R.D.; validation, B.W., R.D. and Y.W.; formal analysis, B.W.; investigation, B.W. and Y.W.; resources, B.W., Y.W., S.N. and Q.J.; data curation, B.W. and R.D.; writing—original draft preparation, B.W.; writing—review and editing, Y.W., R.D., K.S., S.I., S.N. and Q.J.; visualization, B.W. and R.D.; supervision, B.W.; project administration, B.W. and Y.W.; funding acquisition, B.W., R.D. and Y.W. All authors have read and agreed to the published version of the manuscript.

Funding: This research was funded by JSPS KAKENHI, grant numbers JP21K11876 and JP21K17833.

Institutional Review Board Statement: Not applicable.

Data Availability Statement: Not applicable.

Acknowledgments: The authors wish to thank all the workers who participated in the experiments.

Conflicts of Interest: The authors declare no conflict of interest.

References

1. Yasushi, U.; Koujirou, I.; Yuuki, I. Development of Remote Control Paddy Ridge Mower in Nagano Prefecture, System/Control/Information. *Inst. Syst. Control. Inf. Eng.* **2021**, *65*, 471–476. [CrossRef]
2. Iwano, Y. Development of the mowing robot of trimmer type. In Proceedings of the SICE Annual Conference 2010, Taipei, Taiwan, 18–21 August 2010; pp. 1349–1352.
3. Open Access Report, Ministry of Agriculture, Forestry, and Fisheries of Japan, Agriculture and Forestry Census. Available online: https://www.maff.go.jp/j/tokei/sihyo/data/08.html (accessed on 29 May 2022).
4. Ministry of Agriculture, Forestry, and Fisheries. Outline of Agricultural Work Death Accidents that Occurred in 2018. Agricultural Work Fatal Accident Investigation. pp. 1–11. Available online: https://www.maff.go.jp/j/seisan/sien/sizai/s_kikaika/anzen/attach/pdf/index-101.pdf (accessed on 29 May 2022).
5. Ministry of Agriculture, Forestry, and Fisheries. Farm Work Accident That Happened in This Way IV. Investigation of Agricultural Work Accident. p. 41. Available online: http://www.maff.go.jp/j/seisan/sien/sizai/s_kikaika/anzen/23taimen.html (accessed on 29 May 2020).
6. Suenaga, E.; Sumiyoshi, Y.; Takada, S.; Umin, K. Two cases of serious cardiovascular disease found after orthopedic consultation. *Orthop. Surg. Disaster Surg.* **2017**, *66*, 900–903.
7. Wu, B.; Zhu, Y.; Nishimura, S.; Jin, Q. Analyzing the Effects of Driving Experience on Prebraking Behaviors Based on Data Collected by Motion Capture Devices. *IEEE Access* **2020**, *8*, 197337–197351. [CrossRef]
8. Winter, D.A. *Biomechanics and Motor Control of Human Movement*; John Wiley & Sons: Hoboken, NJ, USA, 2009.
9. Bruderlin, A.; Williams, A. Motion signal processing. In Proceedings of the 22nd Annual Conference on Computer Graphics and Interactive Techniques, Los Angeles, CA, USA, 6–11 August 1995.
10. Troje, N.F. Decomposing biological motion: A framework for analysis and synthesis of human gait patterns. *J. Vis.* **2002**, *2*, 371–387. [CrossRef]
11. Aminian, K.; Najaf, B. Capturing human motion using body-fixed sensors: Outdoor measurement and clinical applications. *Comput. Animat. Virtual Worlds* **2004**, *15*, 79–94. [CrossRef]
12. Dong, R.; Cai, D.; Ikuno, S. Motion capture data analysis in the instantaneous frequency-domain using Hilbert–Huang transform. *Sensors* **2020**, *20*, 6534. [CrossRef] [PubMed]
13. Dong, R.; Chen, Y.; Cai, D.; Nakagawa, S.; Higaki, T.; Asai, N. Robot motion design using bunraku emotional expressions—Focusing on Jo-Ha-Kyū in sounds and movements. *Adv. Robot.* **2020**, *34*, 299–312. [CrossRef]

14. Dong, R.; Chang, Q.; Ikuno, S. A deep learning framework for realistic robot motion generation. *Neural Comput. Appl.* **2021**. [CrossRef]
15. Wu, B.; Wu, Y.; Nishimura, S.; Jin, Q. Analysis on the Subdivision of Skilled Mowing Movements on Slopes. *Sensors* **2022**, *22*, 1372. [CrossRef]
16. Wu, B.; Wu, Y.; Aoki, Y.; Nishimura, S. Mowing Patterns Comparison: Analyzing the Mowing Behaviors of Elderly Adults on an Inclined Plane via a Motion Capture Device. *IEEE Access* **2020**, *8*, 216623–216633. [CrossRef]
17. Google. Mediapipe. Available online: https://google.github.io/mediapipe/ (accessed on 29 May 2022).
18. Zhang, S.; Chen, W.; Chen, C.; Liu, Y. Human deep squat detection method based on MediaPipe combined with Yolov5 network. In Proceedings of the 2022 41st Chinese Control Conference (CCC), Hefei, China, 25–27 July 2022; pp. 6404–6409. [CrossRef]
19. Ma, J.; Ma, L.; Ruan, W.; Chen, H.; Feng, J.A. Wushu Posture Recognition System Based on MediaPipe. In Proceedings of the 2022 2nd International Conference on Information Technology and Contemporary Sports (TCS), Guangzhou, China, 24–26 June 2022; pp. 10–13. [CrossRef]
20. Cockcroft, J.; Scheffer, C. Determining the Feasibility of Measuring Outdoor Road Cycling Kinematics Using Inertial Motion Capture Technology. *SAIEE Afr. Res. J.* **2011**, *102*, 31–39. [CrossRef]
21. Wouda, F.J.; Giuberti, M.; Bellusci, G.; Maartens, E.; Reenalda, J.; Van Beijnum BJ, F.; Veltink, P.H. On the Validity of Different Motion Capture Technologies for the Analysis of Running. In Proceedings of the 2018 7th IEEE International Conference on Biomedical Robotics and Biomechatronics (Biorob), Enschede, The Netherlands, 26–29 August 2018; pp. 1175–1180. [CrossRef]
22. Huang, E.N.; Shen, S.S.P. *Hilbert–Huang Transform and Its Applications*, 2nd ed.; World Scientific Publishing: Singapore, 2014.
23. Rilling, G.; Flandrin, P.; Gonçalves, P.; Lilly, J.M. Bivariate empirical mode decomposition. *IEEE Signal Process. Lett.* **2007**, *14*, 936–939. [CrossRef]
24. Rehman, N.; Mandic, D.P. Empirical Mode Decomposition for Trivariate Signals. *IEEE Trans. Signal Process.* **2010**, *58*, 1059–1068. [CrossRef]
25. Rehman, N.; Mandic, D.P. Multivariate empirical mode decomposition. *R. Soc.* **2010**, *466*, 1291–1302. [CrossRef]
26. Bracewell, R.N. *Fourier Transform and Its Applications*; McGraw-Hill Inc Press: New York, NY, USA, 1978.
27. Wu, B.; Zhu, Y.; Dong, R.; Sato, K.; Ikuno, S.; Nishimura, S.; Jin, Q. Pre-braking behaviors analysis based on Hilbert–Huang transform. *CCF Trans. Pervasive Comp. Interact.* **2022**. [CrossRef]
28. Yang, Y.; Hao, F.; Pang, B.; Min, G.; Wu, Y. Dynamic Maximal Cliques Detection and Evolution Management in Social Internet of Things: A Formal Concept Analysis Approach. *IEEE Trans. Netw. Sci. Eng.* **2022**, *9*, 1020–1032. [CrossRef]
29. Hao, F.; Yang, Y.; Mi, G.; Loia, V. Incremental Construction of Three-way Concept Lattice for Knowledge Discovery in Social Networks. *Inf. Sci.* **2021**, *578*, 257–280. [CrossRef]
30. Li, M.; Chen, S.; Chen, X.; Zhang, Y.; Wang, Y.; Tian, Q. Symbiotic graph neural networks for 3d skeleton-based human action recognition and motion prediction. *IEEE Trans. Pattern Anal. Mach. Intell.* **2021**, *44*, 3316–3333. [CrossRef]
31. Zhou, F.; De la Torre, F.; Hodgins, J.K. Hierarchical aligned cluster analysis for temporal clustering of human motion. *IEEE Trans. Pattern Anal. Mach. Intell.* **2012**, *35*, 582–596. [CrossRef]
32. Boashsah, B. Estimating and interpreting the instantaneous frequency of a signal. II. Algorithms and Applications. *Proc. IEEE* **1992**, *80*, 540–568. [CrossRef]
33. Niu, J.; Liu, Y.; Jiang, W.; Li, X.; Kuang, G. Weighted average frequency algorithm for Hilbert–Huang spectrum and its application to micro-Doppler estimation. *IET Radar Sonar Navig.* **2012**, *6*, 595–602. [CrossRef]
34. Dong, R.; Ni, S.; Ikuno, S. Non-linear frequency analysis of COVID-19 spread in Tokyo using empirical mode decomposition. *Sci. Rep.* **2022**, *12*, 2175. [CrossRef] [PubMed]
35. Lee, J. "Hip Height and Sprinting," How to Run Faster . . . at any Age. Part 3. Available online: https://speedendurance.com/2012/01/31/hip-height-and-sprinting/ (accessed on 22 December 2022).
36. Thorpe, S.; Fize, D.; Marlot, C. Speed of processing in the human visual system. *Nature* **1996**, *381*, 520–522. [CrossRef] [PubMed]